

See discussions, stats, and author profiles for this publication at: <https://www.researchgate.net/publication/267508717>

Morphology and Emission Tuning in Fluorescent Nanoparticles Based on Phenylenediacetonitrile

ARTICLE *in* THE JOURNAL OF PHYSICAL CHEMISTRY C · OCTOBER 2014

Impact Factor: 4.77 · DOI: 10.1021/jp507707f

CITATIONS

4

READS

71

7 AUTHORS, INCLUDING:



Eglė Arbačiauskienė
Kaunas University of Technology

14 PUBLICATIONS 66 CITATIONS

[SEE PROFILE](#)



Aurimas Bieliauskas
Kaunas University of Technology

6 PUBLICATIONS 14 CITATIONS

[SEE PROFILE](#)



Vytautas Getautis
Kaunas University of Technology

119 PUBLICATIONS 648 CITATIONS

[SEE PROFILE](#)



Saulius Juršėnas
Vilnius University

146 PUBLICATIONS 1,117 CITATIONS

[SEE PROFILE](#)

Morphology and Emission Tuning in Fluorescent Nanoparticles Based on Phenylenediacetonitrile

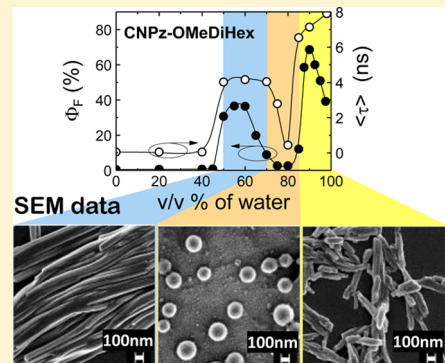
Karolis Kazlauskas,^{*,†} Gediminas Kreiza,[†] Eglė Arbačiauskienė,[‡] Aurimas Bieliauskas,[‡] Vytautas Getautis,[‡] Algirdas Šačkus,[‡] and Saulius Juršėnas[†]

[†]Institute of Applied Research, Vilnius University, Saulėtekio 9-III, Vilnius LT-10222, Lithuania

[‡]Department of Organic Chemistry, Kaunas University of Technology, Radvilėnų pl. 19, Kaunas LT-50254, Lithuania

Supporting Information

ABSTRACT: Organic nanoparticles exhibiting tunable emission properties in response to morphology changes are attractive for application in low-cost fluorescence sensors, e.g., for sensing vapors, temperature, etc., and therefore, convenient ways for altering nanoparticle morphology are highly desired. In this work, phenylenediacetonitrile-based molecules featuring aggregation-induced emission enhancement which are suitable for the realization of morphology-tunable nanoparticles by precipitation method have been designed. The morphology tuning was enabled by rational functionalization of the molecular backbone with pyrazole moieties and adjacent alkoxy/cyclic side-groups, which were varied in size and branchiness. The longer alkoxy chains generally caused formation of crystalline nanostructures, while shorter ones resulted in preferably amorphous nanoaggregates. Remarkably, the sharp tuning of the nanoparticle morphology (crystalline → amorphous → crystalline) with the subsequent high-contrast emission switching (emissive → non emissive → emissive) was achieved for phenylenediacetonitrile bearing dihexylmethoxy-type side-groups by adjusting solvent/nonsolvent ratio ($1/1 \rightarrow 1/4 \rightarrow 1/9$) in the mixture with the dissolved compound. Electron and polarized optical microscopy data confirmed the intermediate non emissive state ($\Phi_F = 2\%$) emanates from amorphous spherical aggregates, whereas two highly emissive states (Φ_F up to 70%) originate from nanowire-like crystalline particles, which were attributed to different phenylenediacetonitrile polymorphs. Finally, the applicability of the phenylenediacetonitrile-based fluorescent nanoparticles for organic vapor sensing was demonstrated.



INTRODUCTION

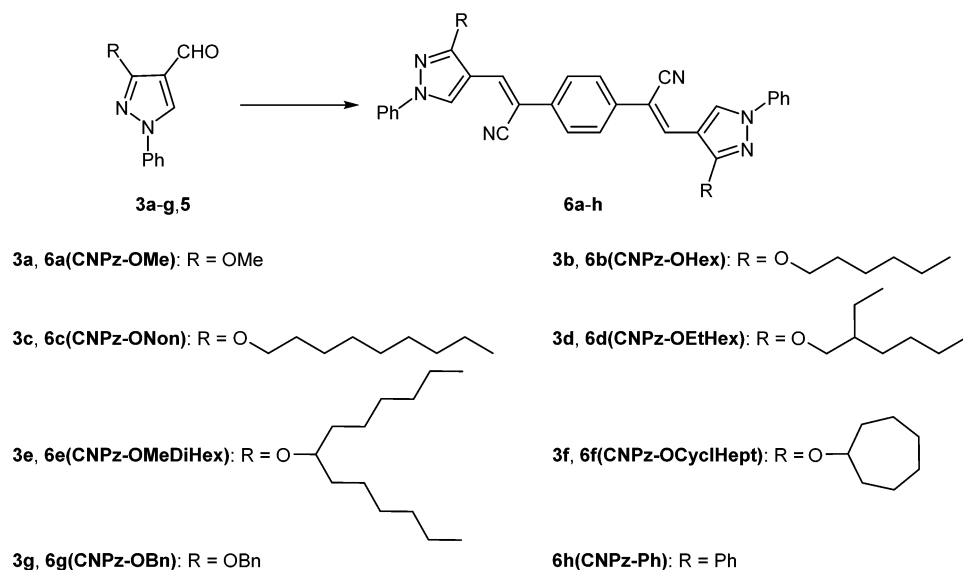
Establishing structure–property relationships and determining the key intramolecular features, which enable molecules to pack into a specific intermolecular pattern capable of performing a desired functionality, are among the most important tasks in materials science. Quite numerous desired organic material properties which are sought to be implemented in optoelectronic devices nowadays can be enabled by modern chemical engineering tools at the molecular level. Aggregation induced emission enhancement (AIEE) is an intriguing material property, which crucially depends on the structure of molecules constituting an aggregated phase, and which has been aimed at by many research groups in order to investigate and even implement AIEE in their own materials or devices.^{1,2} Although the fluorescence enhancement induced by rigid environments or molecule condensation was reported and explained for oligophenylenevinylenes already in 1996,^{3,4} the AIEE phenomenon as such was elaborated and extensively promoted starting from 2001 by studying silole⁵ and cyano-stilbene⁶ compounds. Since the vast majority of known organic fluorophores are fluorescent in the diluted form and almost non emissive in the condensed phase, the discovery of AIEE compounds delivering enhanced emission in the solid state opened a completely new perspective for their utilization in high impact applications like

solid state light emitters,^{7–12} organic lasers,^{13–15} fluorescence sensors (for explosive, ion, pH, temperature, viscosity, pressure detection),^{16,17} bio- and chemosensors,^{7,18} biological probes,¹⁹ etc. For the explanation of AIEE behavior in various types of compounds, different intramolecular and intermolecular mechanisms have been suggested. Suppressed intramolecular torsion/rotation,^{1,20–24} conformational planarization,^{6,25} and restricted intramolecular charge transfer^{12,26} mechanisms, all associated with molecule spatial confinement, were reported to be responsible for the AIEE. On the other hand, intermolecular processes like specific supramolecular stacking architectures (such as in J-aggregates),^{4,27,28} associated with the unique electronic and geometrical properties of the designed molecules or even cooperation of both intramolecular and intermolecular mechanisms,^{6,27,29,30} were also attributed to the significant fluorescence enhancement in the solid state.

The most popular classes of oligomer and polymer compounds claimed to express AIEE behavior are siloles,^{5,16,22,31} distyrylbenzenes,^{29,30,32,33} tetraphenylethenes,^{7,10,18,22} dibenzofulvenes, and cyano-vinylenes.^{6,34} Spe-

Received: July 31, 2014

Revised: October 8, 2014

Scheme 1^a

^aReagents and conditions: 1,4-phenylenediacetonitrile, NaOEt, CHCl₃, rt, overnight, 44–77%.

cial attention has been devoted to the cyano-vinylene-based compounds which exhibit a unique intramolecular feature, twist elasticity, and which are also capable of secondary intermolecular bonding interactions, which both imply realization of various molecular arrangements, and, thus, diverse morphologies in the solid state.^{33,35} Since the performance of functional layers in the molecule-based devices strongly depends on the layer morphology, the possibility of easy morphology tuning is indispensable. Recently, the morphology tuning and the resulting emission switching for AIEE compounds based on diphenyldibenzofulvenes,^{36,37} dicyanodistyrylbenzenes,^{30,35,38} phosphaphhenanthrene,³⁹ arylamines,^{40,41} and others was demonstrated using thermal, mechanical, and volatile organic vapor stimuli. Development of new conformation-tunable stimuli-responsive materials with high emission contrast was recognized to be important for practical applications such as optical memories, functional sensors, optical displays, etc.^{25,30,35,37,38,41–44}

To this end, aiming for AIEE compounds with easy morphology tuning, the series of phenylenediacetonitrile molecules functionalized with pyrazole moieties and various alkoxy or cyclic side-groups was synthesized and investigated. The cyano-vinylene bridges were intentionally introduced into the backbone to provide the twist elasticity along with the AIEE property induced by the sterically demanding cyano groups.^{25,33} The choice of pyrazole moieties was based on their ability to deliver high fluorescence efficiency as well as to cause strong intermolecular hydrogen bondings and π - π interactions important for construction of functional supramolecular structures.^{45,46} The length and the branching degree of alkoxy side chains linked to the pyrazole moiety were chosen to vary for elucidation of the optimal configuration, which in turn could enable simple morphology tuning. The studied compounds were checked for the presence of AIEE behavior by measuring fluorescence efficiency of the compounds dispersed in polymer host as a function of their concentration. Phenylenediacetonitrile nanoparticles formed by precipitation in the solvent/nonsolvent mixture were probed spectroscopically as well as by utilizing fluorescence lifetime and quantum

yield evaluation methods, which in combination with electron and polarized optical microscopy allowed discrimination of the different aggregate morphologies. Remarkably, some of the compounds bearing alkoxy side-groups were found to yield different packing morphologies in the nanoparticles, which could be easily tuned (between crystalline and amorphous) invoking also emission tuning by simply altering solvent/nonsolvent ratio in the mixture.

RESULTS AND DISCUSSION

Synthesis. The studied phenylenediacetonitrile compounds 6a–h, in the text referred to as CNPz-OMe, CNPz-OHex, CNPz-ONon, CNPz-OEtHex, CNPz-OMeDiHex, CNPz-OCyclHept, CNPz-OBn, and CNPz-Ph, respectively, were synthesized using well-known Knoevenagel reaction conditions from the corresponding carbaldehydes 3 and 5 and 1,4-phenylenediacetonitrile in the presence of NaOEt (Scheme 1). For the synthesis of carbaldehydes 3 and 5 see Scheme S1 in the Supporting Information and the details provided therein. The structures of 6a–h were analyzed and identified following the ¹H, ¹³C NMR, IR spectroscopy, mass spectrometry, and elemental analysis data. The full assignment of chemical shifts obtained from the ¹H and ¹³C NMR spectra of compounds 6a–h was based on a combination of standard NMR techniques, such as DEPT, HSQC, HMBC, COSY, TOCSY.

Molecule Geometries Determining Low Emission in Solution. Quantum chemical calculations of the phenylenediacetonitrile derivatives in the gas phase were carried out using density functional theory (DFT) at the B3LYP/6-31G* level as implemented in the Gaussian 09 software package.⁴⁷ Equilibrium ground state geometries of the backbones of all the studied phenylenediacetonitriles were found to be identical irrespective of the side-groups attached. Correspondingly, calculated highest occupied molecular orbital (HOMO) and lowest unoccupied molecular orbital (LUMO) in all the compounds were found to be unperturbed by the side-groups and localized solely on the backbone. Examples of HOMO and LUMO for a few representative compounds CNPz-OMe, CNPz-OMeDiHex, and CNPz-OCyclHept are shown in Figure

S1 in the Supporting Information. The optimized geometry of the selected phenylenediacetonitrile derivative CNPz-OMe as a typical example is illustrated in Figure 1a. For reference, the geometry of analogous compound without cyano groups in the backbone is shown in Figure 1b.

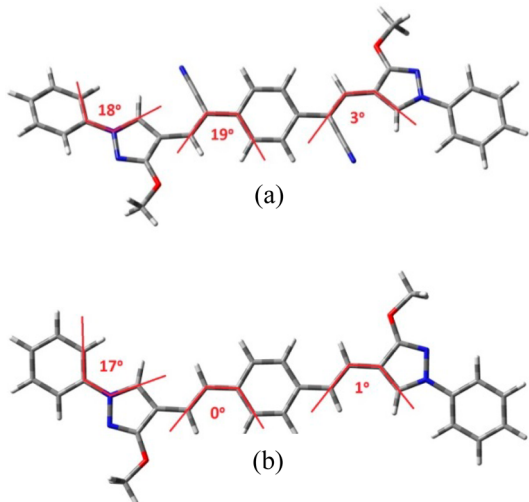


Figure 1. Optimized geometries of the phenylenediacetonitrile derivative CNPz-OMe (a) and the analogous compound without cyano groups (b), as calculated by DFT in the gas phase.

While the backbone of cyano-free compound is planar within the extent of pyrazole moieties, the backbone of dicyano-substituted counterpart is distorted at the vinylene linkages. The distortion of CNPz-OMe backbone at these linkages is somewhat smaller (dihedral angles 19° and 3°) with respect to similar dicyano-substituted distyrylbenzene backbone (dihedral angles 29° and 8°)³³ as a result of less bulky, and, thus, less sterically hindered, pyrazole moieties. Nevertheless, such distortion as well as an additional one induced by the phenyl end-groups forming 18° angle with the pyrazole moieties (see Figure 1a) suffices to promote efficient intramolecular torsions/vibrations like those reported for other cyano-vinylene compounds.^{4,25,26,48} The outcome is an extremely fast non-radiative deactivation of the excited state due to the effective low-frequency vibronic (twist and torsion) mode coupling to the ground state resulting in a very faint emission of the compounds in dilute solutions.^{24,49}

Indeed, the fluorescence quantum yield (Φ_F) of phenylenediacetonitrile compounds in solution is very low and ranges from 0.3% to 0.7% (Figure 2). For alkoxy or cyclic side-groups bridged to the pyrazole moieties via oxygen, Φ_F falls within 0.5–0.7% or is even half as that (0.3%) for CNPz-Ph. Exceptionally low Φ_F of CNPz-Ph is caused by the additional phenyl side-rotors directly linked to the backbone via short methyl bridges. Meanwhile, somewhat longer alkoxy bridges in the rest of the compounds induce smaller steric repulsion, and thus less effectively couple vibronic relaxation. Direct attachment of multiple phenyl-rotors is the base construction element of such well-known AIEE compounds as phenylsiloles^{5,16} and tetraphenylethenes.^{7,50} It ensures extremely low fluorescence in a nonviscous environment. Partial suppression of the intramolecular vibrations, which can be achieved, for example, by anchoring additional phenyl⁵¹ or much heavier carbazolyl⁵² moieties to the labile phenyl end-groups of the phenyl-

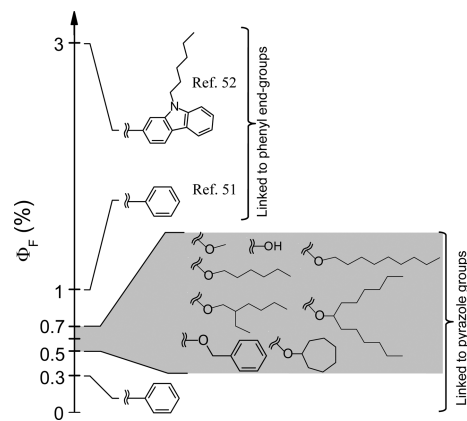


Figure 2. Fluorescence quantum yield of the phenylenediacetonitrile derivatives in 10^{-5} M THF solution as a function of different side-groups (indicated). Data on phenyl and carbazolyl moieties linked to phenyl end-groups of the studied compounds are shown for reference.

enediacetonitrile backbone immediately boosts Φ_F up to 1% or 3%, respectively (see Figure 2).

Concentration Quenching versus AIEE. The presence of AIEE property in the phenylenediacetonitriles was examined by evaluating Φ_F of the compounds dispersed in polystyrene host as a function of their concentration (Figure 3). The evaluation

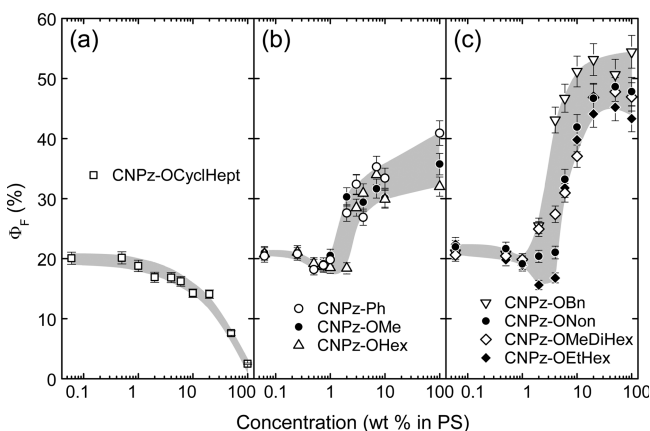


Figure 3. Fluorescence quantum yield of the phenylenediacetonitrile derivatives as a function of their concentration in PS host.

also permitted unambiguous discrimination of the intra- and intermolecular effects determining Φ_F at low and high compound concentration, respectively. Typically, most fluorophores exhibit fluorescence quenching with increasing concentration.^{53–55} This is a result of enhanced excitonic coupling in aggregates significantly reducing radiative decay rate as compared to the rate of competing nonradiative processes, e.g., exciton migration-assisted trapping at the quenching sites (impurities, defects or other imperfections), intersystem crossing to triplet states, etc.⁵⁶ Concentration quenching was observed in phenylenediacetonitrile compound CNPz-OCycl-Hept bearing cycloheptyl side-groups, for which Φ_F was quenched from 20% at low concentrations down to 2% in the neat film (see Figure 3a). Meanwhile, the rest of the compounds expressed pronounced AIEE effect for the concentrations roughly above 2% by weight in PS.

At the lowest compound concentrations in PS host (<1 wt %) all the phenylenediacetonitrile derivatives exhibited $\Phi_F \approx$

21% independently of the side-groups attached. This is almost by 2 orders of magnitude larger as compared to Φ_F values obtained in solution. The Φ_F enlargement in PS host, which occurred solely due to the intramolecular effects, was accompanied by considerable slowing of fluorescence transients with respect to those in solution (see an example for CNPz-OCyclHept in Figure S2 in the Supporting Information) and clearly signified suppression of intramolecular torsions in the environment of increased rigidity. Further Φ_F enhancement with increasing compound concentration above 2 wt % in PS was unambiguously caused by an intermolecular AIEE mechanism, that is, specific molecule stacking likely followed by intramolecular planarization similar to that revealed in cyano-stilbenes.⁵⁷ Electron microscopy and fluorescence microscopy data provided support for such molecule stacking into nanostructures occurring in PS films (see an example for CNPz-OMeDiHex in Figure S3 in the Supporting Information). Interestingly, Φ_F enhancement for some of the side-groups was notably larger (Figure 3c) than for the others (Figure 3b). Mainly the compounds with relatively long and branched side-groups, such as nonyloxy or dihexylmethoxy, demonstrated greater than 2-fold enhancement, from 20% to about 50%, due to the more favorable molecule packing. We note that AIEE could only be achieved for slowly dried PS films, such as those obtained by drop-casting from toluene solution, whereas films prepared by quickly evaporating solvent, e.g., by spin-coating, showed no AIEE behavior. The slow drying was essential in providing extra time necessary for diffusion-driven specific molecule stacking leading to AIEE. Intriguingly, just before manifestation of AIEE, an increase of compound concentration from 0.06 to 2 wt % in PS host caused slight decrease of Φ_F (Figure 3b,c). This decrease could be explained by the absence of critical compound concentration in PS inhibiting proper intermolecular arrangements (necessary for Φ_F enhancement) due to the molecules being too far apart and trapped in between the polymer chains. Disordered molecule arrangements resulted in a usual concentration quenching of fluorescence such as that observed for CNPz-OCyclHept in the whole concentration range 0.06–100 wt % (Figure 3a).

Absorption and Fluorescence Spectroscopy of Phenylendiacetonitrile Nanoparticles. The AIEE effect as a function of the different side-groups was more closely inspected during the process of molecule aggregation, which was accomplished by precipitation of phenylendiacetonitrile nanoparticles in aqueous solution. To elucidate the emission enhancement in the aggregated state and to relate the enhancement with molecular structure, in fact predetermining packing morphology in the aggregates, absorption and fluorescence spectroscopy in combination with fluorescence quantum yield and lifetime measurements were carried out. Three phenylendiacetonitrile compounds bearing cycloheptyloxy (CNPz-OCyclHept), hexyloxy (CNPz-OHex), and dihexylmethoxy (CNPz-OMeDiHex) side-groups and expressing aggregation-caused quenching, moderate and strong AIEE effect, respectively (see Figure 3a–c), were selected as representatives for demonstrating essential differences in their spectroscopic behavior. Figures 4–6 show absorption and fluorescence spectra dynamics of each representative compound in THF/water mixtures with increasing water fraction. Roughly below 50 v/v % of water, absorption and fluorescence spectra of all the studied phenylendiacetonitrile derivatives look identical and are typical of isolated molecules. This is in

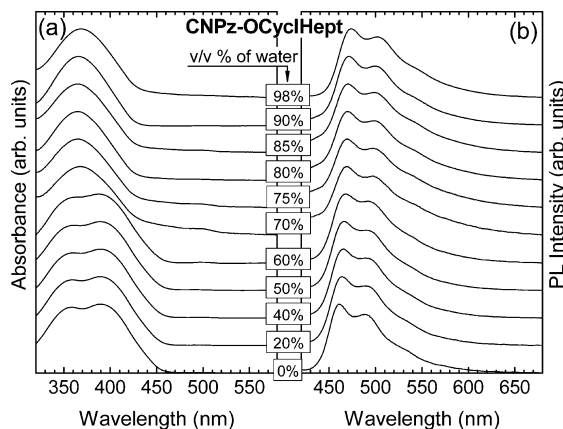


Figure 4. Absorption (a) and fluorescence (b) spectra of CNPz-OCyclHept in THF/water mixture with different volume percent (v/v %) of water. The intensity of each spectrum has been scaled and arbitrarily shifted for clarity.

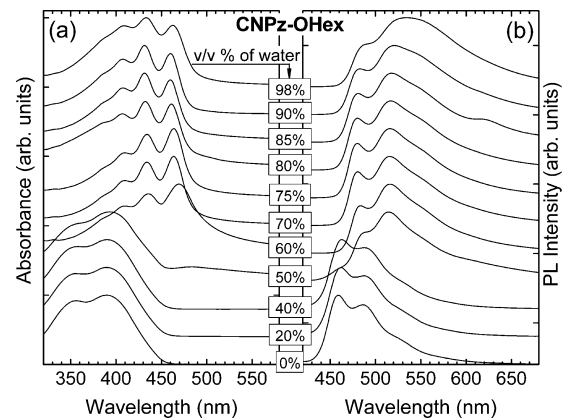


Figure 5. Absorption (a) and fluorescence (b) spectra of CNPz-OHex in THF/water mixture with different volume percent (v/v %) of water. The intensity of each spectrum has been scaled and arbitrarily shifted for clarity.

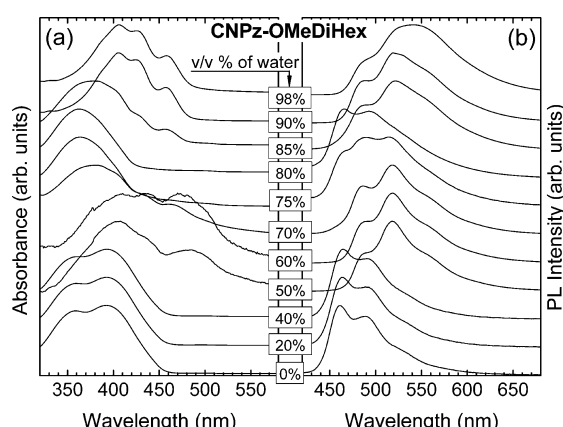


Figure 6. Absorption (a) and fluorescence (b) spectra of CNPz-OMeDiHex in THF/water mixture with different volume percent (v/v %) of water. The intensity of each spectrum has been scaled and arbitrarily shifted for clarity.

agreement with identical HUMOs and LUMOs of the studied derivatives, which were found to be unperturbed by the side-groups (Figure S1 in the Supporting Information).

However, above the limiting water fraction (50 v/v %) separating isolated molecules and formed aggregates (nanoparticles), the spectral dynamics with increasing water content becomes strongly dependent on the side-groups. Namely, CNPz-OCyclHept, above the limiting water fraction, exhibits a single structureless absorption band centered at 370 nm, which remains unchanged up to 98 v/v % of water (Figure 4a). Correspondingly, increasing water fraction negligibly affects fluorescence spectrum of CNPz-OCyclHept up to the largest water fraction (Figure 4b). The spectrum remains very similar to that of isolated molecules, although slight broadening at high water contents can be noticed. Relatively small changes of the spectrum, particularly of the fluorescence spectrum, occurring upon CNPz-OCyclHept aggregation imply weak intermolecular interactions and thus loose molecule packing in the formed nanoparticles. Analogous dynamics was also obtained for CNPz-OEtHex compound bearing ethylhexyloxy side-groups, which justified the importance of rather bulky and branched side-groups for loose packing morphology (see discussion below).

In sharp contrast to CNPz-OCyclHept, the spectral dynamics of CNPz-OHex above 50 v/v % of water indicates an emergence of new absorption band at 470 nm due to aggregates with well-resolved vibronic replicas (Figure 5a). The replicas smoothen at the largest water fractions (>75 v/v %) as another band, in this case broad and structureless, appears in the background at shorter wavelengths (~400 nm) and strengthens in intensity.

A similar tendency is observed in the fluorescence spectra dynamics with increasing water content (Figure 5b). Above the limiting water fraction, the molecular spectrum suddenly transforms into the spectrum of aggregates, which manifests with a new band located at 520 nm. A further increase in the water fraction broadens the aggregate band similarly to that of absorption spectra. The well-expressed vibrational modes of the aggregate band indicate increased rigidity and highly ordered arrangement of the molecules, which are typical of crystalline solids due to strong intermolecular interactions.⁵⁸ Conversely, in amorphous solids due to the absence of long-range periodicity, intermolecular interactions are slightly different at different local sites resulting in the shift of vibronic frequencies, and, consequently, in broadened and washed out spectra. The later features can be traced in the structureless absorption band emerging at about 400 nm.

Importantly, the adjustment of alkoxy chain length was found to enable tuning of the relative intensities of both aggregate bands, i.e., the vibronically modulated absorption band and that with broad and structureless shape. CNPz-OHex and CNPz-ONon compounds with long hexyloxy and nonyloxy side chains expressed analogous dynamics, where aggregate absorption was dominated by vibronically modulated band for all THF/water ratios. In contrast, the structureless aggregate band in the absorption spectra of CNPz-OMe compound bearing short methoxy side-groups overtook domination at the largest water fractions (see Figure S4 in the Supporting Information). This result illustrates that by varying alkoxy side chain length the phenylenediacetonitrile nanoparticles with the different prevalent aggregate state can be obtained. Selective excitation of the vibronically modulated and of the structureless band of CNPz-OHex aggregates formed at 98 v/v % of water yielded similar Φ_F implying efficient energy transfer between the different states. Since the efficient energy transfer is only possible for the states being within the Förster radius (a few

nanometers),⁵⁹ it is likely that the states are intermixed in the aggregates.

Absorption and fluorescence spectra dynamics of CNPz-OMeDiHex bearing branched alkyl side-groups is found to be more complex (Figure 6). In fact certain spectroscopic signatures can be traced back to the two previous compounds.

An increase of the water fraction above 50 v/v % causes the appearance of a new band at about 470 nm in the absorption spectra, and simultaneously, a band at 520 nm in the fluorescence spectra. Although the new absorption band associated with the aggregated phase is rather broad, it still contains discernible vibronic modes. Meanwhile, the new fluorescence band is found to be identical to that of compound CNPz-OHex observed for water fraction above 50 v/v % (Figure 5). Surprisingly, addition of water from 70 v/v % to 85 v/v % gives rise to the new aggregate bands in the absorption and fluorescence spectra, which are very similar to the aggregate bands of compound CNPz-OCyclHept (Figure 4). The absorption band is structureless and centered at 370 nm, whereas the fluorescence band resembles the spectrum of isolated molecules. However, further increase of the water content above 85 v/v % restores the spectra back to those analogous to compound CNPz-OHex. The similarity is particularly obvious for the fluorescence spectra of compounds CNPz-OMeDiHex and CNPz-OHex at the highest water fractions. Thus, spectral dynamics of CNPz-OMeDiHex with increasing water content actually hints on the different aggregate phases (or packing morphologies) formed in accordance to the chosen solvent/nonsolvent ratio in the mixture. Clearly resolved spectroscopic signatures in Figure 6 suggest that three different packing morphologies are formed in the THF/water mixtures for the following water fractions: 50–70 v/v %, 70–85 v/v %, and 85–98 v/v %. Most importantly, the nanoaggregates of different morphologies can be easily realized by utilizing single phenylenediacetonitrile compound functionalized with long and branched dihexylmethoxy-type side chains.

Spectroscopically identified dominating aggregate morphologies along with the extrema Φ_F values for all the studied phenylenediacetonitrile compounds are listed in Table 1. Since the absorption-based measurements permit probing all optically active states including the nonemissive ones, directly inaccessible by fluorescence, the measurements have been chosen as the most suited for evaluation of dominant morphologies.

Table 1 provides evidence that crystalline phase is favored for the compounds featuring long alkoxy side-groups such as CNPz-OHex and CNPz-ONon, whereas purely amorphous phase is inherent for the less structurally regular compounds possessing bulky or branched side-groups like CNPz-OCyclHept and CNPz-OEtHex. Generally, for structurally regular compounds, at relatively low water fraction molecules tend to arrange in an ordered fashion constituting crystalline phase. This is a typical crystallization process driven by molecule diffusion in the bulk.^{60,61} Meanwhile at increased water fraction, and consequently locally increased compound concentration (due to the reduced THF/water ratio), molecule diffusion becomes impossible due to the confined space. This increases the amount of amorphous phase in the nanoparticles of the most compounds (CNPz-OMe, CNPz-OHex, CNPz-ONon, CNPz-OMeDiHex, CNPz-OBn, CNPz-Ph), which is manifested by diminished Φ_F values (see Table 1). However, only for the few compounds (CNPz-OMe and CNPz-Ph) bearing

Table 1. Dominant Morphology and Extrema Φ_F Values of the Phenylenediacetonitrile Nanoparticles As Revealed from the Φ_F and Absorption Spectra Dynamics with Increasing Water Fraction^a

| compd | dominant aggregate morphology (water fraction in THF/water mixture) | extrema values of Φ_F , % |
|----------------|--|--|
| CNPz-OMe | cryst (50–90 v/v %) | 38 @60 v/v % |
| | amorph (90–98 v/v %) | 17 @98 v/v % |
| CNPz-OHex | cryst (50–98 v/v %) | 60 @60 v/v % 20 @98 v/v % |
| CNPz-ONon | cryst (50–98 v/v %) | 32 @60 v/v % 15 @70 v/v % 52 @90 v/v % |
| CNPz-OEtHex | amorph (50–98 v/v %) | 6.0 @98 v/v % |
| CNPz-OCyclHept | amorph (50–98 v/v %) | 6.0 @98 v/v % |
| CNPz-OMeDiHex | cryst (50–70 v/v %) | 40 @60 v/v % |
| | amorph (70–85 v/v %) | 2.0 @80 v/v % |
| | cryst (85–98 v/v %) | 70 @90 v/v % |
| CNPz-OBn | cryst (50–98 v/v %) | 41 @70 v/v % 18 @85 v/v % |
| CNPz-Ph | cryst (50–90 v/v %) | 30 @85 v/v % |
| | amorph (90–98 v/v %) | 8.0 @98 v/v % |

^aPercentage error of QY values is 5%.

relatively small side-groups does the amorphous phase prevail over crystalline at the largest water fractions. The most unusual case is that of CNPz-OMeDiHex (discussed above), with the crystalline ordering being the dominant one at low water fraction (~60 v/v %), and yet surpassed by the amorphous phase at somewhat higher water fraction (~80 v/v %), until it starts dominating again at the highest water fraction (>90 v/v %). This intricate phenomenon is discussed below.

Fluorescence Quantum Yield and Lifetime Dynamics of Phenylenediacetonitrile-Based Nanoparticles. Figure 7 depicts Φ_F and fluorescence lifetime dynamics of the three representative compounds CNPz-OCyclHept, CNPz-OHex, and CNPz-OMeDiHex in THF/water mixture with increasing water content. The presence of noninteracting molecule species below 50 v/v % of water implies geometrically unrestricted relaxation to the ground state via low-frequency intramolecular torsions/vibrations resulting in nearly zero Φ_F and extremely short excited state lifetime (<70 ps). Although the limitations of our experimental setup do not permit evaluation of shorter τ , such τ values can be assumed to be zero in the nanosecond time scale within the accuracy of 7%.

Generally, nanoparticle precipitation initiated by the increased water fraction promoted AIEE in all the phenylenediacetonitrile compounds. However, the AIEE effect was found to be relatively small for the compound CNPz-OCyclHept exhibiting concentration quenching in PS host (Figure 7a).

For this compound Φ_F was enhanced by only an order of magnitude, from 0.6% to 6%. The small AIEE complied with the weak intermolecular interactions in the nanoparticles revealed from the spectra dynamics (Figure 4a). On the

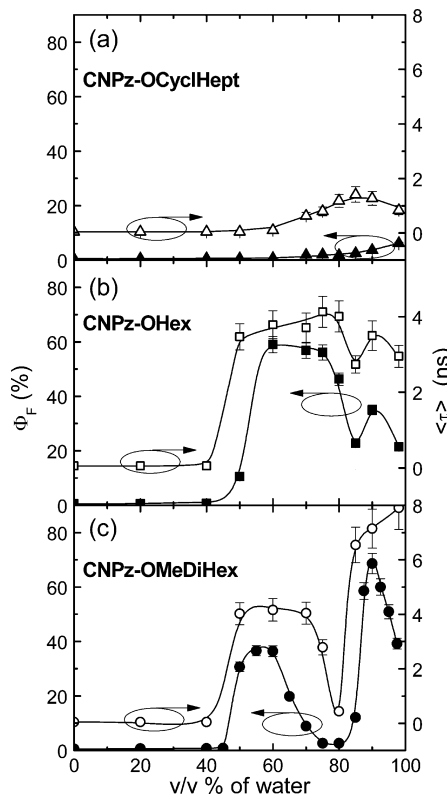


Figure 7. Fluorescence quantum yield (solid points) and average fluorescence lifetime (white points) of CNPz-OCyclHept (a), CNPz-OHex (b), and CNPz-OMeDiHex (c) as a function of volume percent (v/v %) of water in THF/water mixture. Zero point of the $\langle \tau \rangle$ axis has been arbitrarily shifted for clarity.

other hand, the AIEE was much more profound for the rest of the phenylenediacetonitrile derivatives. In this case, Φ_F was enhanced by almost 2 orders of magnitude, from 0.6% to 40% and above. The examples of remarkable AIEE are illustrated in Figure 7b,c for CNPz-OHex and CNPz-OMeDiHex, respectively. Interestingly, here Φ_F behavior with increasing water fraction is found to be nonmonotonous. In the case of CNPz-OHex, Φ_F first increases up to 60% at the 60–75 v/v % of water and then decreases down to 20% above 75 v/v % of water (Figure 7b). Note that the latter decrease is consistent with the concomitant growth of unstructured slope at ~400 nm in the absorption spectra (Figure 5a). Variations in fluorescence intensity accompanied by changes in color upon nanoparticle formation are highlighted in the pictures of the THF/water mixtures with increasing water fraction (see Figure S5 in the Supporting Information). In the case of CNPz-OMeDiHex, an increase of Φ_F up to 40% at the 50–60 v/v % of water is followed by the steep decrease of Φ_F down to 2% at the 75–80 v/v % of water, and then again, sudden increase of Φ_F up to 70% at about 90 v/v % of water, which is followed by rapid decrease of Φ_F above 90 v/v % of water (Figure 7c). Such wavy Φ_F profile agrees well with the complex spectra dynamics of compound CNPz-OMeDiHex shown in Figure 6. Particularly, each boost in Φ_F is accompanied by the appearance of new aggregate bands enriched with vibronic modes and red-shifted with respect to molecular spectra. Meanwhile, the drop in Φ_F is followed by the emergence of structureless aggregate band located at the shorter wavelengths.

The distinctive Φ_F behaviors with increasing water content were reflected in the excited state relaxation dynamics of the

phenylenediacetonitriles revealed from fluorescence transients. The transients of a few representative compounds CNPz-OCyclHept and CNPz-OMeDiHex at different water fractions are displayed in Figure 8. Fluorescence transients of the rest of

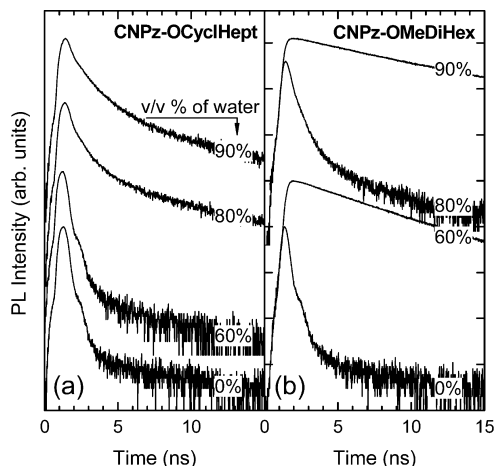


Figure 8. Fluorescence transients of CNPz-OCyclHept (a) and CNPz-OMeDiHex (b) in THF/water mixtures with different volume percent (v/v %) of water. The intensity of each transient has been scaled and arbitrarily shifted for clarity.

the phenylenediacetonitriles are provided in Figure S6 in the Supporting Information. Estimated average fluorescence lifetimes (τ) are depicted in Figure 7. The rapid fluorescence decay observed for the isolated CNPz-OCyclHept molecules in solution (below 50 v/v % of water) gradually slows down upon molecule aggregation (above 50 v/v % of water) as a result of increasing restriction of intramolecular motions.

The relatively weak and gradual changes of the lifetime are associated with rather weak intermolecular interactions in CNPz-OCyclHept aggregates due to the bulky cycloheptyloxy side-groups. The bulky groups prevent tight molecule packing into special patterns in the nanoparticles, which disallows complete suppression of vibrational/torsional relaxation modes responsible for fast excited state deactivation. In sharp contrast, the rapid fluorescence decay of CNPz-OMeDiHex molecules in solution is abruptly slowed down upon aggregate formation resulting in a remarkable increase of τ up to 4 ns at 60 v/v % of water. An addition of water fraction up to 80 v/v % gives rise to the aggregates showing subnanosecond relaxation time, whereas further increase of the water content up to 90 v/v % immediately restores the τ back to the nanosecond time scale again. Such abrupt variations of the lifetime are likely associated with the dramatic changes in molecule packing morphology, and also with suppression or permission of vibrational/torsional relaxation, thus enabling fluorescence on–off switching. These distinct attributes of radically different molecular arrangements of CNPz-OCyclHept and CNPz-OMeDiHex (or CNPz-OHex or CNPz-ONon) are also easily traced from the direct comparison of their fluorescence spectra and transients obtained in solution and solid state (see Figure S7 in the Supporting Information). Note that independent estimates of average fluorescence lifetimes nicely follow Φ_F and spectra dynamics with increasing water content, what confirms reliability of the experimental data and strengthens the argument about the existence of different aggregate morphologies, which can be tuned by simply altering solvent (THF) to nonsolvent (water) ratio in THF/water mixture.

Electron and Polarized Optical Microscopy of Nanoparticles. Scanning electron microscopy (SEM) and polarized optical microscopy (POM) were employed to visualize phenylenediacetonitrile nanoparticles, and, additionally, to confirm the different packing morphologies, which were indirectly revealed from the fluorescence quantum yield, lifetime, and spectral dynamics. SEM images of CNPz-OCyclHept, CNPz-OEtHex, and CNPz-OBn nanoparticles prepared in the THF/water mixtures with 90 v/v % of water and casted on precleaned silicon substrates are shown in Figure 9a,c,e. The images indicate a spherical shape of the nano-

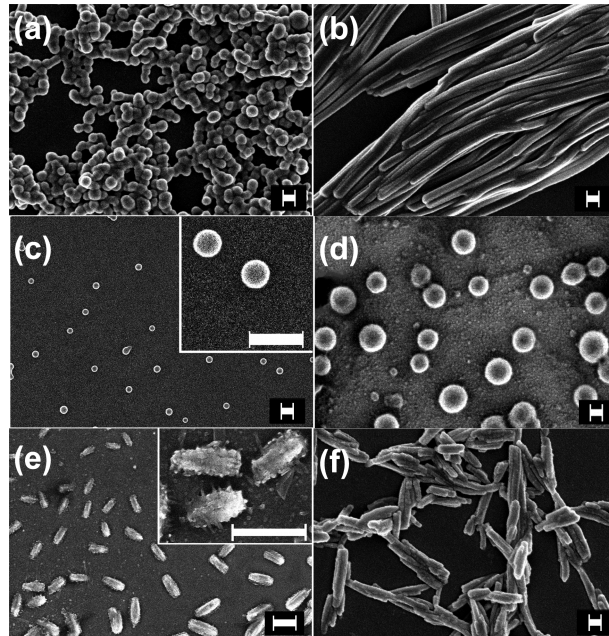


Figure 9. Electron microscopy images of CNPz-OCyclHept (a), CNPz-OEtHex (c), CNPz-OBn (e) nanoparticles formed in THF/water mixtures with 90 v/v % of water and CNPz-OMeDiHex nanoparticles formed in the mixtures with 60 (b), 80 (d), and 90 (f) v/v % of water. The scale bar for (a, b, c, d, f) is 100 nm and for (e) is 500 nm.

particles with mean diameters of about 50 nm for CNPz-OCyclHept and CNPz-OEtHex (Figure 9a,c), which demonstrate structureless spectral bands of the aggregates due to random and loose molecule packing.

On the other hand, CNPz-OBn nanoparticles have rather intricate shape (see Figure 9e and the inset). They are seen to be composed of many nanoneedles of a well-defined shape. Clearly resolved vibronic modes in the absorption spectra of nanoneedles suggest crystalline morphology as a dominant one (Table 1). Reducing water fraction down to 60 v/v % is found to cause a continuous increase in the nanoparticle sizes up to about 1 μ m. The size tunability in the submicron range was confirmed *in situ* in the THF/water mixtures by dynamic light scattering (DLS) technique (see Figure S8 in the Supporting Information and explanations therein). Note that the correct estimation of nanoparticle sizes by DLS was only possible for CNPz-OCyclHept and CNPz-OEtHex compounds forming spherical particles due to the limitations of evaluation method used. The technique tends to overestimate actual particle diameters, which is more noticeable for the smaller nanoparticles. The DLS measurements also indicated that additional size tuning can be achieved via altering compound concen-

tration in the mixture. A decrease in nanoparticle diameter with decreasing compound concentration has been clearly evidenced.

SEM images of CNPz-OMeDiHex nanoparticles prepared at different water fractions demonstrate drastic differences in aggregate size and shape (Figure 9b,d,f). Highly fluorescent aggregates formed at 60 and 90 v/v % of water have a shape of long and short nanowire-like structures, respectively. The long nanowires are about 6 μm in length and have a mean diameter of 80 nm, whereas the short ones are 50 nm in diameter and at most 500 nm in length. The smaller nanowires exhibit almost twice as high fluorescence efficiency ($\Phi_F = 70\%$) as compared to the longer ones ($\Phi_F = 40\%$), which is likely due to the different molecule packing. Attempts to reveal packing morphology in the nanowires by X-rays diffraction were unsuccessful due to an inability to obtain larger crystals; however, different absorption bands, different fluorescence lifetimes, and efficiencies associated with the longer and shorter nanowires hinted that different molecular packing is indeed very probable. Interestingly, poorly fluorescent ($\Phi_F = 2\%$) CNPz-OMeDiHex nanoaggregates formed at 80 v/v % of water and expressing structureless spectral bands have spherical shape with a mean diameter of about 150 nm.

To confirm the amorphous nature of round aggregates and crystalline morphology of the nanowire-like particles, polarized optical microscopy (POM) experiments were carried out (Figure 10).

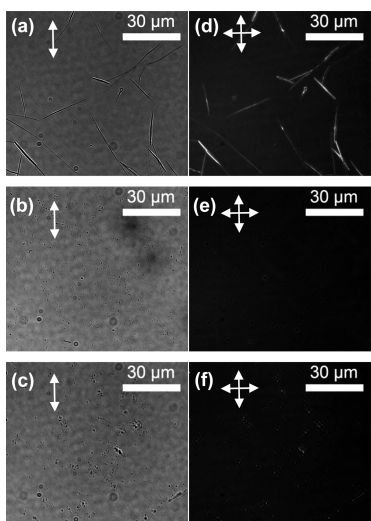


Figure 10. Polarized optical microscopy images of the CNPz-OMeDiHex nanoparticles formed in the THF/water mixtures with 60 (a, d), 80 (b, e), and 90 v/v % (c, f) of water under parallel (a–c) and crossed (d–f) polarizers.

Long and short nanowire-like aggregates equally nicely discernible under parallel and crossed polarizers (compare Figure 10a with d and c with f) imply strong birefringence, which unambiguously indicates their crystallinity. Conversely, a completely dark optical image of the round nanoparticles observed under crossed polarizers (compare Figure 10b with e) signifies the absence of birefringence, and is a signature of their amorphous nature. Unfortunately, it was impossible to resolve particles with diameter smaller than 400 nm (the case of Figure 10b, c, e, and f) due to the limitations imposed by optical diffraction; nevertheless, somewhat enlarged aggregates as dark

(bright) spots under parallel (crossed) polarizers could still be clearly discerned.

Thus, POM results support previously discussed SEM and spectroscopic data, which imply facile tuning of the nanoparticle morphology (crystalline \rightarrow amorphous \rightarrow crystalline) and the corresponding emission switching (emissive \rightarrow non emissive \rightarrow emissive) with a maximum contrast of over 30 achieved for CNPz-OMeDiHex by adjusting solvent/nonsolvent ratio in the mixture. While the appearance of non emissive amorphous phase with the increasing water fraction (i.e., decreasing THF/water ratio) can be naturally understood by the inhibition of diffusion-driven ordered molecule packing due to spatial constraints, the reappearance of the crystalline phase at the highest water fractions (for THF/water ratio $<1/9$) is rather unusual. To our knowledge, such intricate nanoparticle morphology dynamics governed by solvent/nonsolvent ratio has not been observed yet. The reappearance of the crystalline phase in diffusionless conditions at high molecule concentration can be explained by the surfaced-enhanced crystallization phenomenon,^{62–64} which becomes increasingly important with the reduced nanoparticle size, and thus increased surface to volume ratio. The phenomenon implies much faster growth of the crystals from amorphous phase on the surface than in the interior and is sustained by enhanced surface diffusion. Moreover, highly fluorescent nanocrystallites formed at THF/water ratio $<1/9$ constitute a different polymorph as compared to that formed at the ratio of 1/1. The different polymorphs can be justified by the different spectral bands ascribed in the absorption spectra (Figure 6) as well as by the distinct fluorescence lifetimes and quantum yields (Figure 7). Remarkably, such sharp alteration of nanoparticle morphology accompanied by high-contrast variation in emission efficiency is facilitated by long and branched dihexylmethoxy-type of side chains. The other studied alkoxy or cyclic side-groups have either failed to achieve such sharp morphology tuning or the tuning was marginal.

Vapor Sensing by Fluorescent Nanoparticles. For a simple demonstration of the applicability of the phenylenediacetonitrile nanoparticles in vapor sensing, the compound CNPz-OMeDiHex with Φ_F of up to 70% and the compound CNPz-OCyclHept with Φ_F of only up to 6% in the aggregated state were used. Amorphous neat films of CNPz-OMeDiHex and CNPz-OCyclHept were prepared on the glass substrates from solution by quickly evaporating the solvent (Figures 11a and 12a).

The absence of crystallinity of the as-prepared films was confirmed by the fluorescence spectrum, which was found to be similar to the spectrum of the compounds in a dilute solution. Exposure of the defined area of the CNPz-OMeDiHex film to THF vapor for a few seconds resulted in a sudden change of the color of that area from greenish-blue to vivid yellowish-green. A close inspection of the exposed area by using a fluorescence microscope revealed highly fluorescent fiber-like particles with a submicron diameter (Figure 11b). The nanoparticles were confirmed to be crystalline from their fluorescence spectra, which were identical to those of the long nanowire-like aggregates formed in THF/water mixture at 50–60 v/v % of water. The formation of the crystalline nanowires was obviously caused by a sudden drop in a viscosity of the rigid surroundings due to the penetration of solvent vapor into the film, which facilitated diffusion-driven ordering of the molecules into crystalline nanoparticles. The formed crystalline particles were

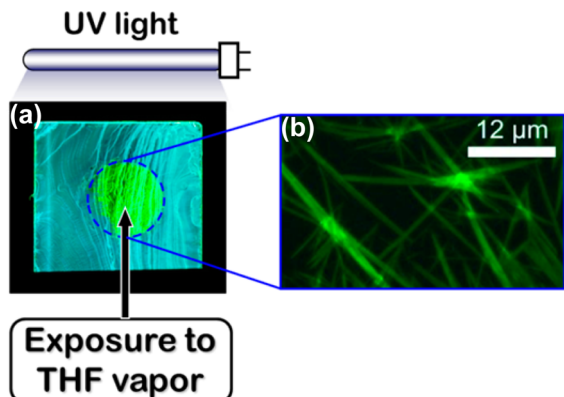


Figure 11. Fluorescence image of the neat CNPz-OMeDiHex film with the highlighted area exposed to THF vapor (a). Fluorescence microscopy image of the highlighted area (b). The images were taken under UV excitation.

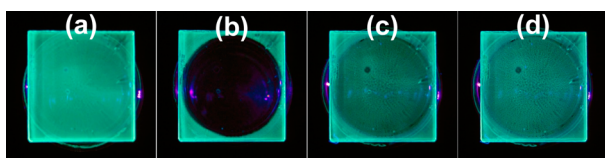


Figure 12. Fluorescence image of the neat CNPz-OCyclHept film under UV excitation and before exposure (a), 0 s after exposure (b), 10 s after exposure (c), and 30 min after exposure (d) to THF vapor. The images b, c, and d were taken with THF vapor stimulus removed.

found to be very stable, implying that such a sensor based on the amorphous-to-crystalline phase changes is irreversible.

Unlike for CNPz-OMeDiHex, exposure of amorphous neat film of CNPz-OCyclHept to THF vapor did not result in a color change, but rather caused fluorescence quenching (Figure 12a,b).

Formation of highly crystalline nanoparticles in this case was precluded by the bulky cycloheptyloxy side-groups, which conditioned weak intermolecular interactions, and, therefore, favored dissolution over association. The fluorescence quenching was related to the lessened suppression of intramolecular torsions due to the vapor-induced solubilization of the film. The exposed area of fluorescent amorphous film could be recovered to a large degree under ambient conditions after removing THF vapor stimulus and letting the film dry for a few minutes (Figure 12c,d).

Thus, the above demonstrations clearly show the applicability of the phenylenediacetonitrile-based compounds for unassisted eye sensing of volatile organic vapor via distinct change in fluorescence color or intensity.

CONCLUSIONS

In conclusion, phenylenediacetonitrile-based fluorescent nanoparticles with tunable morphology and emission properties were demonstrated. The tuning in the nanoparticles formed by simple precipitation technique was realized via adjusting solvent/nonsolvent ratio in the mixture with the dissolved compound. Functionalization of the twisted phenylenediacetonitrile backbone with pyrazole and various peripheral alkoxy/cyclic moieties facilitated manipulation of packing morphology resulting in either crystalline nanostructures (in the case of long alkoxy side moieties) or amorphous spherical particles (in the case of shorter side moieties). Crystalline and amorphous

phases were clearly discerned by their spectroscopic signatures, fluorescence quantum yield, and lifetime behaviors and later confirmed by SEM and polarized optical microscopy. Of the tested compounds with various peripheral groups, the long and branched dihexylmethoxy side-groups were found to be optimal in achieving sharp morphology and emission tuning in the phenylenediacetonitrile nanoparticles. Particularly, the emission quantum yield could be tuned from 40% down to 2% and up to 70% in correspondence with the morphology changes crystalline → amorphous → crystalline by adjusting THF/water ratio from 1/1 to 1/4 and to 1/9 in the mixture with the dissolved compound. Two highly emissive states formed at THF/water ratio of 1/1 and 1/9 were associated with crystalline nanowire-like particles originating from different phenylenediacetonitrile polymorphs. Finally, THF vapor sensing via distinct change in emission color or intensity was demonstrated implying potential application of the fluorescent phenylenediacetonitrile nanoparticles in volatile vapor sensors.

ASSOCIATED CONTENT

S Supporting Information

Synthesis information, instrumentation and methods, HOMO and LUMO orbitals, fluorescence transients, SEM and fluorescence microscopy data, absorption and fluorescence spectra, pictures of the compounds in THF/water mixtures under UV excitation, and DLS data on size distributions of nanoparticles. This material is available free of charge via the Internet at <http://pubs.acs.org>.

AUTHOR INFORMATION

Corresponding Author

*Phone: +370 5 2366032. Fax: +370 5 2366059. E-mail: karolis.kazlauskas@ff.vu.lt.

Notes

The authors declare no competing financial interest.

ACKNOWLEDGMENTS

This research was supported by the European Social Fund under the Global Grant measure. G.K. acknowledges support by project "Promotion of Student Scientific Activities" (VP1-3.1-ŠMM-01-V-02-003) from the Research Council of Lithuania. S. Šakirzanovas is acknowledged for SEM measurements.

REFERENCES

- (1) Hong, Y.; Lam, J. W. Y.; Tang, B. Z. Aggregation-Induced Emission: Phenomenon, Mechanism and Applications. *Chem. Commun.* **2009**, 4332–4353.
- (2) Hong, Y.; Lam, J. W. Y.; Tang, B. Z. Aggregation-Induced Emission. *Chem. Soc. Rev.* **2011**, *40*, 5361–5388.
- (3) Oelkrug, D.; Tompert, A.; Egelhaaf, H.; Hanack, M.; Steinhuber, E.; Hohloch, M.; Meier, H.; Stalmach, U. Towards Highly Luminescent Phenylene Vinylene Films. *Synth. Met.* **1996**, *83*, 231–237.
- (4) Oelkrug, D.; Tompert, A.; Gierschner, J.; Egelhaaf, H. J.; Hanack, M.; Hohloch, M.; Steinhuber, E. Tuning of Fluorescence in Films and Nanoparticles of Oligophenylenevinylenes. *J. Phys. Chem. B* **1998**, *102*, 1902–1907.
- (5) Luo, J.; Xie, Z.; Lam, J. W. ; Cheng, L.; Tang, B. Z.; Chen, H.; Qiu, C.; Kwok, H. S.; Zhan, X.; Liu, Y. Aggregation-Induced Emission of 1-Methyl-1,2,3,4,5-Pentaphenylsilole. *Chem. Commun.* **2001**, *2001*, 1740–1741.
- (6) An, B. K.; Kwon, S. K.; Jung, S. D.; Park, S. Y. Enhanced Emission and Its Switching in Fluorescent Organic Nanoparticles. *J. Am. Chem. Soc.* **2002**, *124*, 14410–14415.

- (7) Dong, Y.; Lam, J. W. Y.; Qin, A.; Liu, J.; Li, Z.; Tang, B. Z.; Sun, J.; Kwok, H. S. Aggregation-Induced Emissions of Tetraphenylethene Derivatives and Their Utilities as Chemical Vapor Sensors and in Organic Light-Emitting Diodes. *Appl. Phys. Lett.* **2007**, *91*, 011111.
- (8) Ning, Z.; Chen, Z.; Zhang, Q.; Yan, Y.; Qian, S.; Cao, Y.; Tian, H. Aggregation-Induced Emission (AIE)-Active Starburst Triarylamine Fluorophores as Potential Non-Doped Red Emitters for Organic Light-Emitting Diodes and Cl₂ Gas Chemodosimeter. *Adv. Funct. Mater.* **2007**, *17*, 3799–3807.
- (9) Yuan, W. Z.; Lu, P.; Chen, S.; Lam, J. W. Y.; Wang, Z.; Liu, Y.; Kwok, H. S.; Ma, Y.; Tang, B. Z. Changing the Behavior of Chromophores from Aggregation-Caused Quenching to Aggregation-Induced Emission: Development of Highly Efficient Light Emitters in the Solid State. *Adv. Mater.* **2010**, *22*, 2159–2163.
- (10) Zhao, Z.; Chen, S.; Lam, J. W. Y.; Lu, P.; Zhong, Y.; Wong, K. S.; Kwok, H. S.; Tang, B. Z. Creation of Highly Efficient Solid Emitter by Decorating Pyrene Core with AIE-Active Tetraphenylethene Peripheries. *Chem. Commun.* **2010**, *46*, 2221–2223.
- (11) Chan, C. Y. K.; Zhao, Z.; Lam, J. W. Y.; Liu, J.; Chen, S.; Lu, P.; Mahtab, F.; Chen, X.; Sung, H. H. Y.; Kwok, H. S.; et al. Efficient Light Emitters in the Solid State: Synthesis, Aggregation-Induced Emission, Electroluminescence, and Sensory Properties of Luminogens with Benzene Cores and Multiple Triarylvinylic Peripherals. *Adv. Funct. Mater.* **2012**, *22*, 378–389.
- (12) Yuan, W. Z.; Gong, Y.; Chen, S.; Shen, X. Y.; Lam, J. W. Y.; Lu, P.; Lu, Y.; Wang, Z.; Hu, R.; Xie, N.; et al. Efficient Solid Emitters with Aggregation-Induced Emission and Intramolecular Charge Transfer Characteristics: Molecular Design, Synthesis, Photophysical Behaviors, and OLED Application. *Chem. Mater.* **2012**, *24*, 1518–1528.
- (13) Tanaka, M.; Oki, Y.; Nagano, D.; An, B.-K.; Park, S. Y.; Maeda, M. Distributed Feedback Waveguide Laser of Organic Nano-Compound Material. *Mol. Cryst. Liq. Cryst.* **2007**, *463*, 173/[455]–183/[465].
- (14) Cheng, K. H.; Zhong, Y.; Xie, B. Y.; Dong, Y. Q.; Hong, Y.; Sun, J. Z.; Tang, B. Z.; Wong, K. S. Fabrication of and Ultraviolet Lasing in TPE/PMMA Polymer Nanowires. *J. Phys. Chem. C* **2008**, *112*, 17507–17511.
- (15) Fang, H.-H.; Chen, Q.-D.; Yang, J.; Xia, H.; Gao, B.-R.; Feng, J.; Ma, Y.-G.; Sun, H.-B. Two-Photon Pumped Amplified Spontaneous Emission from Cyano-Substituted Oligo(p-Phenylenevinylene) Crystals with Aggregation-Induced Emission Enhancement. *J. Phys. Chem. C* **2010**, *114*, 11958–11961.
- (16) Li, Z.; Dong, Y. Q.; Lam, J. W. Y.; Sun, J.; Qin, A.; Häußler, M.; Dong, Y. P.; Sung, H. H. Y.; Williams, I. D.; Kwok, H. S.; et al. Functionalized Siloles: Versatile Synthesis, Aggregation-Induced Emission, and Sensory and Device Applications. *Adv. Funct. Mater.* **2009**, *19*, 905–917.
- (17) Wu, J.; Liu, W.; Ge, J.; Zhang, H.; Wang, P. New Sensing Mechanisms for Design of Fluorescent Chemosensors Emerging in Recent Years. *Chem. Soc. Rev.* **2011**, *40*, 3483–3495.
- (18) Wang, M.; Zhang, G.; Zhang, D.; Zhu, D.; Tang, B. Z. Fluorescent Bio/Chemosensors Based on Silole and Tetraphenylethene Luminogens with Aggregation-Induced Emission Feature. *J. Mater. Chem.* **2010**, *20*, 1858–1867.
- (19) Ding, D.; Li, K.; Liu, B.; Tang, B. Z. Bioprobe Based on AIE Fluorogens. *Acc. Chem. Res.* **2013**, *46*, 2441–2453.
- (20) He, J.; Xu, B.; Chen, F.; Xia, H.; Li, K.; Ye, L.; Tian, W. Aggregation-Induced Emission in the Crystals of 9,10-Distyrylbenzene Derivatives: The Essential Role of Restricted Intramolecular Torsion. *J. Phys. Chem. C* **2009**, *113*, 9892–9899.
- (21) Feng, X.; Tong, B.; Shen, J.; Shi, J.; Han, T.; Chen, L.; Zhi, J.; Lu, P.; Ma, Y.; Dong, Y. Aggregation-Induced Emission Enhancement of Aryl-Substituted Pyrrole Derivatives. *J. Phys. Chem. B* **2010**, *114*, 16731–16736.
- (22) Qin, A.; Lam, J. W. Y.; Tang, B. Z. Luminogenic Polymers with Aggregation-Induced Emission Characteristics. *Prog. Polym. Sci.* **2012**, *37*, 182–209.
- (23) Kazlauskas, K.; Miasojedovas, A.; Dobrovolskas, D.; Arbačiauskienė, E.; Getautis, V.; Šačkus, A.; Juršėnas, S. Self-Assembled Nanoparticles of P-Phenylenediacetonitrile Derivatives with Fluorescence Turn-On. *J. Nanopart. Res.* **2012**, *14*, 877–890.
- (24) Shustova, N. B.; Ong, T.-C.; Cozzolino, A. F.; Michaelis, V. K.; Griffin, R. G.; Dincă, M. Phenyl Ring Dynamics in a Tetraphenylethylene-Bridged Metal–Organic Framework: Implications for the Mechanism of Aggregation-Induced Emission. *J. Am. Chem. Soc.* **2012**, *134*, 15061–15070.
- (25) An, B.-K.; Gierschner, J.; Park, S. Y. π-Conjugated Cyanostilbene Derivatives: A Unique Self-Assembly Motif for Molecular Nanostructures with Enhanced Emission and Transport. *Acc. Chem. Res.* **2012**, *45*, 544–554.
- (26) Gao, B.-R.; Wang, H.-Y.; Hao, Y.-W.; Fu, L.-M.; Fang, H.-H.; Jiang, Y.; Wang, L.; Chen, Q.-D.; Xia, H.; Pan, L.-Y.; et al. Time-Resolved Fluorescence Study of Aggregation-Induced Emission Enhancement by Restriction of Intramolecular Charge Transfer State. *J. Phys. Chem. B* **2010**, *114*, 128–134.
- (27) An, B. K.; Lee, D. S.; Lee, J. S.; Park, Y. S.; Song, H. S.; Park, S. Y. Strongly Fluorescent Organogel System Comprising Fibrillar Self-Assembly of a Trifluoromethyl-Based Cyanostilbene Derivative. *J. Am. Chem. Soc.* **2004**, *126*, 10232–10233.
- (28) Dai, Q.; Liu, W.; Zeng, L.; Lee, C. S.; Wu, J.; Wang, P. Aggregation-Induced Emission Enhancement Materials with Large Red Shifts and Their Self-Assembled Crystal Microstructures. *CrystEngComm* **2011**, *13*, 4617–4624.
- (29) Bhongale, C. J.; Chang, C.-W.; Lee, C.-S.; Diau, E. W.-G.; Hsu, C.-S. Relaxation Dynamics and Structural Characterization of Organic Nanoparticles with Enhanced Emission. *J. Phys. Chem. B* **2005**, *109*, 13472–13482.
- (30) Yoon, S.-J.; Chung, J. W.; Gierschner, J.; Kim, K. S.; Choi, M.-G.; Kim, D.; Park, S. Y. Multistimuli Two-Color Luminescence Switching via Different Slip-Stacking of Highly Fluorescent Molecular Sheets. *J. Am. Chem. Soc.* **2010**, *132*, 13675–13683.
- (31) Chen, J.; Law, C. C. W.; Lam, J. W. Y.; Dong, Y.; Lo, S. M. F.; Williams, I. D.; Zhu, D.; Tang, B. Z. Synthesis, Light Emission, Nanoaggregation, and Restricted Intramolecular Rotation of 1,1-Substituted 2,3,4,5-Tetraphenylsiloles. *Chem. Mater.* **2003**, *15*, 1535–1546.
- (32) Xie, Z.; Yang, B.; Xie, W.; Liu, L.; Shen, F.; Wang, H.; Yang, X.; Wang, Z.; Li, Y.; Hanif, M.; et al. A Class of Nonplanar Conjugated Compounds with Aggregation-Induced Emission: Structural and Optical Properties of 2,5-Diphenyl-1,4-Distyrylbenzene Derivatives with All Cis Double Bonds. *J. Phys. Chem. B* **2006**, *110*, 20993–21000.
- (33) Gierschner, J.; Park, S. Y. Luminescent Distyrylbenzenes: Tailoring Molecular Structure and Crystalline Morphology. *J. Mater. Chem. C* **2013**, *1*, 5818–5832.
- (34) Chang, C. W.; Bhongale, C. J.; Lee, C. S.; Huang, W. K.; Hsu, C. S.; Diau, E. W. G. Relaxation Dynamics and Structural Characterization of Organic Nanobelts with Aggregation-Induced Emission. *J. Phys. Chem. C* **2012**, *116*, 15146–15154.
- (35) Yoon, S. J.; Park, S. Y. Polymorphic and Mechanochromic Luminescence Modulation in the Highly Emissive Dicyanodistyrylbenzene Crystal: Secondary Bonding Interaction in Molecular Stacking Assembly. *J. Mater. Chem.* **2011**, *21*, 8338–8346.
- (36) Luo, X.; Li, J.; Li, C.; Heng, L.; Dong, Y. Q.; Liu, Z.; Bo, Z.; Tang, B. Z. Reversible Switching of the Emission of Diphenyldibenzofulvenes by Thermal and Mechanical Stimuli. *Adv. Mater.* **2011**, *23*, 3261–3265.
- (37) Gu, X.; Yao, J.; Zhang, G.; Yan, Y.; Zhang, C.; Peng, Q.; Liao, Q.; Wu, Y.; Xu, Z.; Zhao, Y.; et al. Polymorphism-Dependent Emission for Di(p-Methoxyphenyl)dibenzofulvene and Analogues: Optical Waveguide/Amplified Spontaneous Emission Behaviors. *Adv. Funct. Mater.* **2012**, *22*, 4862–4872.
- (38) Chung, J. W.; You, Y.; Huh, H. S.; An, B.-K.; Yoon, S.-J.; Kim, S. H.; Lee, S. W.; Park, S. Y. Shear- and UV-Induced Fluorescence Switching in Stilbene II-Dimer Crystals Powered by Reversible [2 + 2] Cycloaddition. *J. Am. Chem. Soc.* **2009**, *131*, 8163–8172.
- (39) Qian, L.; Tong, B.; Shen, J.; Shi, J.; Zhi, J.; Dong, Y.; Yang, F.; Dong, Y.; Lam, J. W. Y.; Liu, Y.; et al. Crystallization-Induced Emission

- Enhancement in a Phosphorus-Containing Heterocyclic Luminogen. *J. Phys. Chem. B* **2009**, *113*, 9098–9103.
- (40) Gong, Y.; Tan, Y.; Liu, J.; Lu, P.; Feng, C.; Yuan, W. Z.; Lu, Y.; Sun, J. Z.; He, G.; Zhang, Y. Twisted D–π–A Solid Emitters: Efficient Emission and High Contrast Mechanochromism. *Chem. Commun.* **2013**, *49*, 4009–4011.
- (41) Zhang, Y.; Sun, J.; Zhuang, G.; Ouyang, M.; Yu, Z.; Cao, F.; Pan, G.; Tang, P.; Zhang, C.; Ma, Y. Heating and Mechanical Force-Induced Luminescence On–Off Switching of Arylamine Derivatives with Highly Distorted Structures. *J. Mater. Chem. C* **2014**, *2*, 195–200.
- (42) Sagara, Y.; Kato, T. Mechanically Induced Luminescence Changes in Molecular Assemblies. *Nat. Chem.* **2009**, *1*, 605–610.
- (43) Grzelczak, M.; Vermant, J.; Furst, E. M.; Liz-Marzán, L. M. Directed Self-Assembly of Nanoparticles. *ACS Nano* **2010**, *4*, 3591–3605.
- (44) Kunzelman, J.; Crenshaw, B. R.; Weder, C. Self-Assembly of Chromogenic Dyes—A New Mechanism for Humidity Sensors. *J. Mater. Chem.* **2007**, *17*, 2989–2991.
- (45) Zhang, H. Y.; Zhang, Z. L.; Ye, K. Q.; Zhang, J. Y.; Wang, Y. Organic Crystals with Tunable Emission Colors Based on a Single Organic Molecule and Different Molecular Packing Structures. *Adv. Mater.* **2006**, *18*, 2369–2372.
- (46) Willy, B.; Mueller, T. J. J. Regioselective Three-Component Synthesis of Highly Fluorescent 1,3,5-Trisubstituted Pyrazoles. *Eur. J. Org. Chem.* **2008**, *2008*, 4157–4168.
- (47) Frisch, M. J.; Trucks, G. W.; Schlegel, H. B.; Scuseria, G. E.; Robb, M. A.; Cheeseman, J. R.; Scalmani, G.; Barone, V.; Mennucci, B.; Petersson, G. A.; et al. *Gaussian 09, Revision D. 01*; Gaussian, Inc.: Wallingford, CT, 2009.
- (48) Belletête, M.; Morin, J.-F.; Leclerc, M.; Durocher, G. A Theoretical, Spectroscopic, and Photophysical Study of 2,7-Carbazolevinylene-Based Conjugated Derivatives. *J. Phys. Chem. A* **2005**, *109*, 6953–6959.
- (49) Peng, Q.; Yi, Y.; Shuai, Z.; Shao, J. Toward Quantitative Prediction of Molecular Fluorescence Quantum Efficiency: Role of Duschinsky Rotation. *J. Am. Chem. Soc.* **2007**, *129*, 9333–9339.
- (50) Zhao, Z.; Chen, S.; Shen, X.; Mahtab, F.; Yu, Y.; Lu, P.; Lam, J. W. Y.; Kwok, H. S.; Tang, B. Z. Aggregation-Induced Emission, Self-Assembly, and Electroluminescence of 4,4'-bis(1,2,2-Triphenylvinyl)-biphenyl. *Chem. Commun.* **2010**, *46*, 686–688.
- (51) Arbačiauskienė, E.; Kazlauskas, K.; Miasojedovas, A.; Juršėnas, S.; Jankauskas, V.; Holzer, W.; Getautis, V.; Šačkus, A. Pyrazolyl-Substituted Polyconjugated Molecules for Optoelectronic Applications. *Dyes Pigm.* **2010**, *85*, 79–85.
- (52) Arbačiauskienė, E.; Kazlauskas, K.; Miasojedovas, A.; Juršėnas, S.; Jankauskas, V.; Holzer, W.; Getautis, V.; Šačkus, A. Multifunctional Polyconjugated Molecules with Carbazolyl and Pyrazolyl Moieties for Optoelectronic Applications. *Synth. Met.* **2010**, *160*, 490–498.
- (53) Miasojedovas, A.; Kazlauskas, K.; Armonaitė, G.; Sivamurugan, V.; Valiyaveettil, S.; Grazulevicius, J. V.; Jursenas, S. Concentration Effects on Emission of Bay-Substituted Perylene Diimide Derivatives in a Polymer Matrix. *Dyes Pigm.* **2012**, *92*, 1285–1291.
- (54) Krotkus, S.; Kazlauskas, K.; Miasojedovas, A.; Gruodis, A.; Tomkeviciene, A.; Grazulevicius, J. V.; Jursenas, S. Pyrenyl-Functionalized Fluorene and Carbazole Derivatives as Blue Light Emitters. *J. Phys. Chem. C* **2012**, *116*, 7561–7572.
- (55) Karpicz, R.; Puzinas, S.; Krotkus, S.; Kazlauskas, K.; Jursenas, S.; Grazulevicius, J. V.; Grigalevicius, S.; Gulbinas, V. Impact of Intramolecular Twisting and Exciton Migration on Emission Efficiency of Multifunctional Fluorene-Benzothiadiazole-Carbazole Compounds. *J. Chem. Phys.* **2011**, *134*, 204508–204516.
- (56) Gierschner, J.; Lüer, L.; Milián-Medina, B.; Oelkrug, D.; Egelhaaf, H.-J. Highly Emissive H-Aggregates or Aggregation-Induced Emission Quenching? The Photophysics of All-Trans Para-Distyrylbenzene. *J. Phys. Chem. Lett.* **2013**, *4*, 2686–2697.
- (57) An, B. K.; Gihm, S. H.; Chung, J. W.; Park, C. R.; Kwon, S. K.; Park, S. Y. Color-Tuned Highly Fluorescent Organic Nanowires/nanofabrics: Easy Massive Fabrication and Molecular Structural Origin. *J. Am. Chem. Soc.* **2009**, *131*, 3950–3957.
- (58) Taliani, C. In *Organic Nanostructures: Science and Applications*; Agranovich, V. M., La Rocca, G. C., Eds.; IOS Press: Amsterdam, 2002; pp 187–228.
- (59) Förster, T. 10th Spiers Memorial Lecture. Transfer Mechanisms of Electronic Excitation. *Discuss. Faraday Soc.* **1959**, *27*, 7–17.
- (60) Sun, Y.; Xi, H.; Chen, S.; Ediger, M. D.; Yu, L. Crystallization near Glass Transition: Transition from Diffusion-Controlled to Diffusionless Crystal Growth Studied with Seven Polymorphs. *J. Phys. Chem. B* **2008**, *112*, 5594–5601.
- (61) Gnutzmann, T.; Rademann, K.; Emmerling, F. Fast Crystallization of Organic Glass Formers. *Chem. Commun.* **2012**, *48*, 1638–1640.
- (62) Wu, T.; Yu, L. Surface Crystallization of Indomethacin Below T *G*. *Pharm. Res.* **2006**, *23*, 2350–2355.
- (63) Gunn, E.; Guzei, I.; Yu, L. Does Crystal Density Control Fast Surface Crystal Growth in Glasses? A Study with Polymorphs. *Cryst. Growth Des.* **2011**, *11*, 3979–3984.
- (64) Hasebe, M.; Musumeci, D.; Powell, C. T.; Cai, T.; Gunn, E.; Zhu, L.; Yu, L. Fast Surface Crystal Growth on Molecular Glasses and Its Termination by the Onset of Fluidity. *J. Phys. Chem. B* **2014**, *118*, 7638–7646.